Title

Evolutionary and functional analyses reveal a role for the RHIM in tuning RIPK3 activity across vertebrates

Authors

Elizabeth J. Fay[1], Kolya Isterabadi[1], Charles M. Rezanka[1], Jessica Le[1], Matthew D. Daugherty[1]*

Affiliations

[1]Department of Molecular Biology, School of Biological Sciences, University of California, San Diego, La Jolla, CA, 92093

* To whom correspondence should be addressed: Matthew D. Daugherty (mddaugherty@ucsd.edu)

Abstract

Receptor interacting protein kinases (RIPK) RIPK1 and RIPK3 play important roles in diverse innate immune pathways. Despite this, some RIPK1/3-associated proteins are absent in specific vertebrate lineages, suggesting that some RIPK1/3 functions are conserved while others are more evolutionarily labile. Here, we perform comparative evolutionary analyses of RIPK1-5 and associated proteins in vertebrates to identify lineage-specific rapid evolution of RIPK3 and RIPK1 and recurrent loss of RIPK3-associated proteins. Despite this, diverse vertebrate RIPK3 proteins are able to activate NF-κB and cell death in human cells. Additional analyses revealed a striking conservation of the RIP homotypic interaction motif (RHIM) in RIPK3, as well as other human RHIM-containing proteins. Interestingly, diversity in the RIPK3 RHIM can tune activation of NF-κB while retaining the ability to activate cell death. Altogether, these data suggest that NF-κB activation is a core, conserved function of RIPK3, and the RHIM can tailor RIPK3 function to specific needs within and between species.

Introduction

Receptor interacting protein kinase 3 (RIPK3), and the closely related kinase RIPK1, have critical roles in mediating cell death and inflammatory signaling [1]. Downstream of signals from innate immune receptors like Z-DNA binding protein 1 (ZBP1) and tumor necrosis factor receptor 1 (TNFR1), RIPK3 and RIPK1 interact via their shared RIP homotypic interaction motif (RHIM), leading to their autophosphorylation and activation of additional effector proteins to carry out their innate immune functions. For example, RIPK3 can phosphorylate MLKL to activate highly inflammatory programmed necrotic cell death (necroptosis) [2], RIPK1/3 can engage caspase-8 (CASP8) to activate apoptotic caspases [3, 4], or RIPK1/3 can activate the pro-survival and pro-inflammatory transcription factor NF-κB [5, 6]. Several factors are known to impact the outcome of RIPK1/3 activation, such as the activating signal and caspase activity [1, 7]. Altogether, RIPK3 and RIPK1 are central to determining cell fate downstream of various innate immune stimuli.

Like many innate immune proteins, RIPK3 is evolutionarily dynamic in vertebrates. Phylogenomic analyses of a small number of species from different vertebrate clades suggest that RIPK3, and the associated proteins ZBP1 and MLKL, have been lost in some vertebrate lineages including birds, carnivores, and marsupials [8, 9]. In addition, RIPK3, RIPK1, MLKL, and ZBP1 are known to interact with viral proteins [10-15] and have been shown to be evolving under recurrent positive selection in both primates and bats [16, 17], a hallmark of host proteins that directly interact with viral proteins [18]. Despite the known evolutionary divergence of RIPK3 in vertebrates, most of what is known about their activation and regulation is from studies conducted in humans and mice. Even between humans and mice, there are known differences in the roles of specific genes in regulation of NF-κB, suggesting this pathway can be tailored to the distinct environments of different species [19]. These differences likely extend beyond humans and mice, and likely include RIPK1/RIPK3 mediated activation of NF-κB. Furthermore, RIPK1 and RIPK3 are part of a larger family of RIPKs, including RIPK2, RIPK4, and ANKK1/RIPK5, which, with the exception of RIPK5, are known to activate NF-κB in various cellular contexts [20-22]. The

62 degree to which these other RIP kinases and their interacting partners have diversified
63 across vertebrates is unknown.

64 Here, we use evolutionary and functional approaches to characterize
65 diversification of RIPK3-mediated activation of NF-κB. We identified RIPK1- and RHIM-
66 mediated activation of NF-κB by diverse vertebrate RIPK3 proteins, as well as distinct
67 mechanisms of RIPK3-mediated activation of NF-κB. Phylogenetic and phylogenomic
68 analyses of RIPK1-5 and several key associated proteins revealed the dynamic evolution
69 of RIPK3 and RIPK1. In addition to observing the loss of RIPK3 and necroptosis-
70 associated proteins in some vertebrate lineages, we identify changes in regulatory
71 features—including catalytic sites and CASP cleavage sites—in RIPK3 and RIPK1 in
72 specific mammalian lineages that may affect their function. Intriguingly, we found that the
73 RHIM domain of RIPK3 and RIPK1, as well as other RHIM-containing proteins, is highly
74 conserved in vertebrates and in a non-vertebrate RIPK1 protein. Consistent with this
75 strong conservation of the RHIM domain, we found that RIPK1 proteins from diverse
76 vertebrates, and even a non-vertebrate RIPK1, are able to activate NF-κB, suggesting
77 that activation of this inflammatory response is a conserved function of RIPK3, RIPK1,
78 and potentially other RHIM-containing proteins in vertebrates. Altogether, these data
79 suggest that activation of NF-κB is the ancestral and conserved feature of RIPK3 and
80 RIPK1, while other functions such as necroptosis are more evolutionarily labile and
81 rapidly evolving, likely as a response to evolutionary pressure from pathogens.

82

83 **Results**

84 *Comparative evolutionary analysis of RIPK1-5*

85 To understand the evolution and diversification of RIPK function, we first wished to
86 compare the functions of human RIPKs. There are canonically four RIPKs in humans,
87 RIPK1-4. ANKK1 is a close paralog of RIPK4 and has therefore been denoted as RIPK5.
88 Additional proteins have also been described as RIPK proteins, including DSTYK,
89 LRRK1, and LRRK2, but these proteins are phylogenetically distinct and will therefore not
90 be considered here [22]. The shared domain architecture of RIPK1-5 includes a
91 conserved N-terminal kinase domain, an extended disordered intermediate domain, and
92 distinct protein interaction domains at the C-terminus that can include a death domain

93 (DD), RIP homotypic interaction motif (RHIM), caspase activation and recruitment domain
94 (CARD), or ankyrin repeats (ANK) (Figure 1A). Human RIPK1-4 activate NF-κB, albeit
95 through different mechanisms, including differential dependence on endogenous RIPK1
96 and kinase activity (Supplementary Figure 1-3). Interestingly, despite its close homology
97 to RIPK4, RIPK5 did not activate NF-κB. Altogether, these data highlight NF-κB as a
98 shared function of RIPK1-4.

99 We next wished to perform comparative evolutionary analyses of RIPK1-5 in
100 vertebrates to determine which RIPKs might be undergoing functional divergence. We
101 first analyzed RIPK1-5 in four distinct mammalian clades to determine whether there was
102 evidence of recurrent positive selection, which can be a hallmark of host-pathogen
103 interactions and can drive functional diversification. Notably, we only found evidence for
104 positive selection acting on RIPK1 and RIPK3 (Fig 1B, Supplementary files 1-2).
105 Interestingly, RIPK1 and RIPK3 are not uniformly evolving under positive selection in all
106 mammalian clades analyzed. For instance, in primates, RIPK3 is evolving under strong
107 positive selection, where RIPK1 is not, consistent with previous data [16, 17]. In contrast,
108 ungulate RIPK3 does not show evidence for positive selection whereas ungulate RIPK1
109 does. These data indicate that among RIPK1-5, only RIPK1 and RIPK3 genes have
110 undergone recurrent positive selection, and that RIPK1 and RIPK3 may have faced
111 different selective pressures across distinct mammalian lineages.

112 In addition to evolving under positive selection in primates and bats [16], RIPK3,
113 ZBP1, and MLKL are known to be lost in some vertebrate lineages [8]. However, it is
114 unknown if other RIPK and RIPK-associated proteins are similarly lost. We therefore
115 performed phylogenomic analysis on 489 vertebrate species for the presence or absence
116 of RIPK1-5 and several key RIPK-associated proteins (Figure 1C, Supplementary Files 4
117 and 5). Due to the difficulty in discerning whether a gene absence in an individual species
118 is due to true gene loss or incomplete genome assembly, we focused on multi-species
119 patterns of gene loss within and between vertebrate lineages. Given that NF-κB is broadly
120 present in many vertebrate and non-vertebrate species, including horseshoe crab [23],
121 *Drosophila melanogaster* [24], and cnidarians and bivalves (reviewed in [25]), we
122 analyzed proteins associated with other RIPK functions. We first confirmed the loss of
123 necroptosis associated proteins that has been previously reported [8]: RIPK3 and ZBP1

124 in birds; RIPK3, ZBP1, and MLKL in marsupials; MLKL in carnivores. In addition, we found
125 that ZBP1 is absent in all fish species, suggesting that this protein, and ZBP1-mediated
126 necroptosis, arose only during tetrapod evolution.

127 We then analyzed RIPK1 and its associated proteins. RIPK1 is found nearly every
128 vertebrate genome queried, as well as clear homologs in several non-vertebrate species,
129 including zebra mussel (*Dreissena polymorpha*). Additional RIPK-like proteins have been
130 found in other non-vertebrate species, including a RIPK1/2-like protein in *Drosophila* and
131 other protostomes [8], although these proteins were not considered here due to minimal
132 sequence similarity to the human RIP kinase domains and our focus on vertebrate RIP
133 kinases. Likewise, caspase-8 (CASP8), a known regulator of RIPK1, is found in most
134 tetrapod genomes, although it is absent in fish and sea lamprey. This emergence of
135 CASP8 in tetrapods coincides with the emergence of ZBP1 in tetrapods. Further
136 supporting the link between CASP8 and ZBP1, CASP8 is lost in some reptiles that have
137 also lost ZBP1 (Supplementary Table 1). CASP8 is a known negative regulator of
138 necroptosis and is important for mitigating ZBP1-induced inflammation [26]. These data
139 suggest that loss of ZBP1 is sufficient to allow for loss of CASP8. In contrast to CASP8,
140 its close paralog, CASP10 is present in fish and sea lamprey but displays patterns of
141 lineage specific loss. For example, we confirmed the loss of CASP10 in some rodents
142 [27], revealing that suborder Myomorpha ("mouse-like") and Castorimorpha ("beaver-
143 like") rodents have lost CASP10, whereas Sciuromorpha ("squirrel-like") and
144 Hystricomorpha ("porcupine-like") rodents have retained CASP10. We also found loss of
145 CASP10 in all marsupials and several ungulates. Finally, we found that FADD and TRIF
146 are well conserved in all vertebrates.

147 We also analyzed the phylogenomic distribution of RIPK2, 4, and 5 and their
148 associated proteins. RIPK2 and its associated protein NOD1 are found in most
149 vertebrates [20, 21]. Intriguingly, we observed a second paralog of RIPK2, which we call
150 RIPK2B, in many vertebrates but lost in therian (live-bearing) mammals (Supplementary
151 Figure 4). NOD2 is present in lamprey and fish, but absent in birds, reptiles, and some
152 amphibians, including some of the same species that contain RIPK2B. While RIPK2B
153 retains both the kinase domain and CARD, there may be distinct regulatory mechanisms,
154 specifically those related to NOD2, compared to RIPK2. RIPK4 is present in jawed

155 vertebrates. IRF6, the only known phosphorylation target of RIPK4 [20, 21], emerged prior
156 to RIPK4 and has been lost in many vertebrate species, particularly in carnivores,
157 cetaceans, and ungulates. RIPK5, which has no known function and no known interacting
158 proteins, has been lost in several lineages, including monotremes and lagomorphs.
159 Overall, our analyses revealed that RIPK1 and RIPK3 are evolutionarily distinct from other
160 RIP kinases, and the recurrent loss of some RIPK1/3-associated necroptosis proteins
161 (ZBP1, MLKL, CASP8) and RIPK3 suggests that these proteins may have functions
162 tailored to the needs of specific vertebrate lineages.

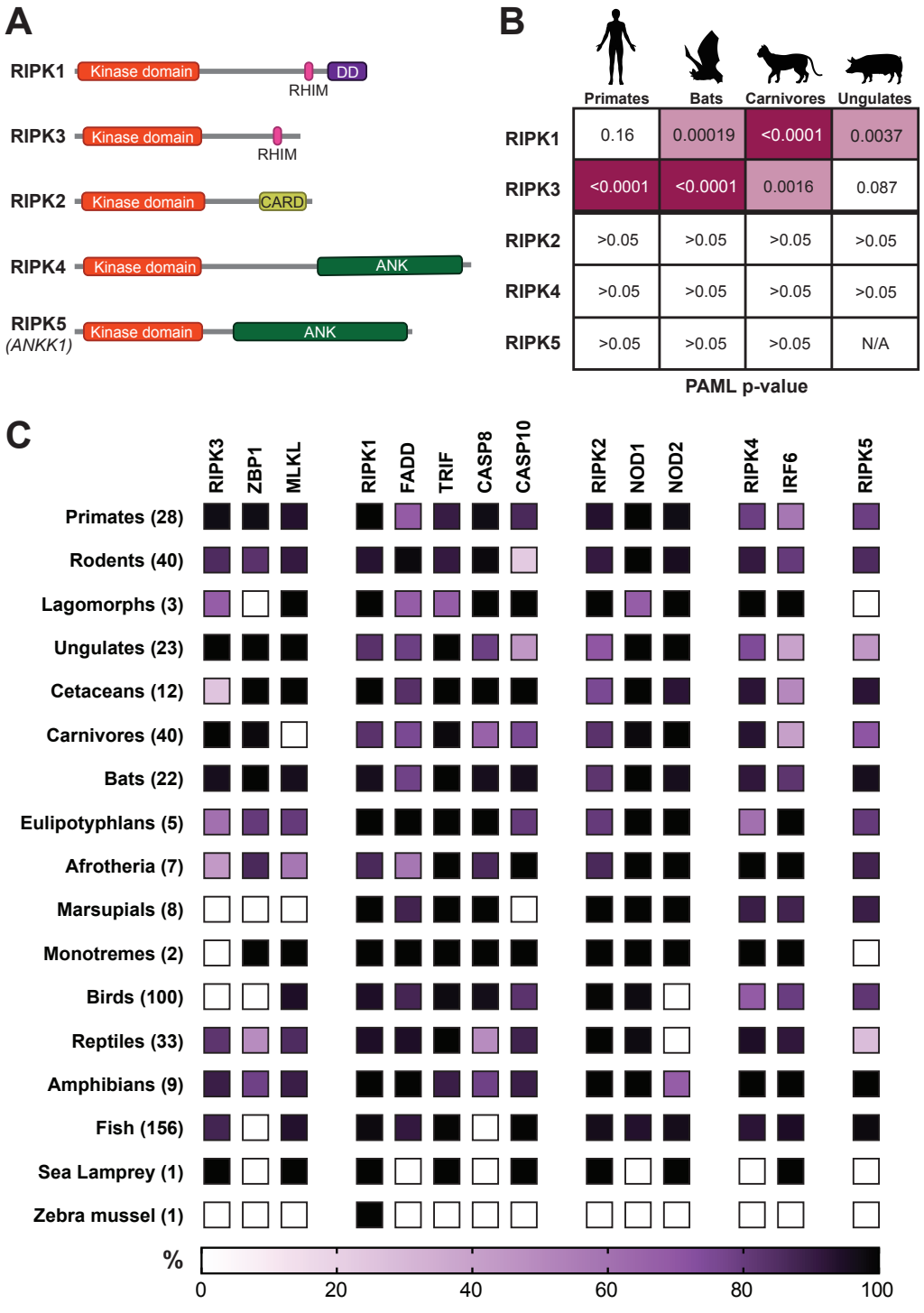

Figure 1. Comparative evolutionary analysis of RIPK1-5. (A) Domain structures of human RIP kinases. RHIM = RIP homotypic interaction motif, DD = death domain, CARD = caspase activation and recruitment domain, ANK = ankyrin repeats. (B) Positive selection analysis of RIPK1-5 in the indicated mammalian order. Input sequences and PAML p-values can be found in Supplementary Files 1 and 2. Images of model species generated using BioRender. (C) Heat amp showing the percentage of species within a clade that have the indicated protein. The clades and the number of species within each clade are indicated on the left. Complete lists of proteins and species in each group can be found in Supplementary Files 4 and 5.

172 *Diverse vertebrate RIPK3 proteins activate NF-κB*

173 Our analyses revealed dynamic evolution of RIPK3 in vertebrates, including
174 signatures of positive selection in multiple mammalian clades and recurrent loss of RIPK3
175 and its associated proteins. We hypothesized that this rapid RIPK3 evolution may have
176 resulted in different functions of RIPK3 in different vertebrate lineages. We therefore
177 tested the ability of RIPK3 proteins from diverse vertebrates, ranging from 23-63%
178 similarity to humans (Fig 2A, Supplementary Figure 5), to activate NF-κB in human cells.
179 To our surprise, among all vertebrates tested, including mammals, reptiles, and sea
180 lamprey, only pig and sea lamprey RIPK3 failed to activate NF-κB in human cells (Fig
181 2B). This striking conservation of function indicates that NF-κB activation has remained
182 intact despite lineage specific RIPK3 divergence and loss of interacting partners. We then
183 analyzed whether, like human RIPK3 (Supplementary Figure 1C) [28], other vertebrate
184 RIPK3 proteins require RIPK1 to activate NF-κB by repeating experiments in RIPK1 KO
185 cells. Interestingly, while mammalian RIPK3 activation is dependent on RIPK1, both lizard
186 and turtle RIPK3 activate NF-κB independently of RIPK1 (Fig 2B). These results indicate
187 that the requirements for NF-κB activation by RIPK3 are species-specific.

188 Finally, we tested whether another function of RIPK3, activation of ZBP1- and
189 MLKL-dependent cell death (Supplementary Figure 6), is also conserved. Most
190 mammalian RIPK3 proteins were able to activate cell death using human ZBP1 and MLKL
191 (Fig 2C). This included pig RIPK3, which is unable to activate NF-κB, suggesting that
192 activation of cell death and NF-κB by RIPK3 proteins have been separated in a species-
193 specific manner. Likewise, we observed that cat RIPK3 can activate NF-κB but fails to
194 activate cell death. Based on this observation, we analyzed the sequences of carnivore
195 RIPK3 proteins and found that feline RIPK3 have mutated kinase catalytic residue
196 (Supplementary Figure 7), explaining the loss of cell death activation by cat RIPK3.
197 Outside of mammals, only lizard RIPK3 was able to activate cell death, despite the ability
198 of both lizard and turtle RIPK3 to activate NF-κB, further suggesting that these functions
199 of RIPK3 have distinct, species-specific requirements.

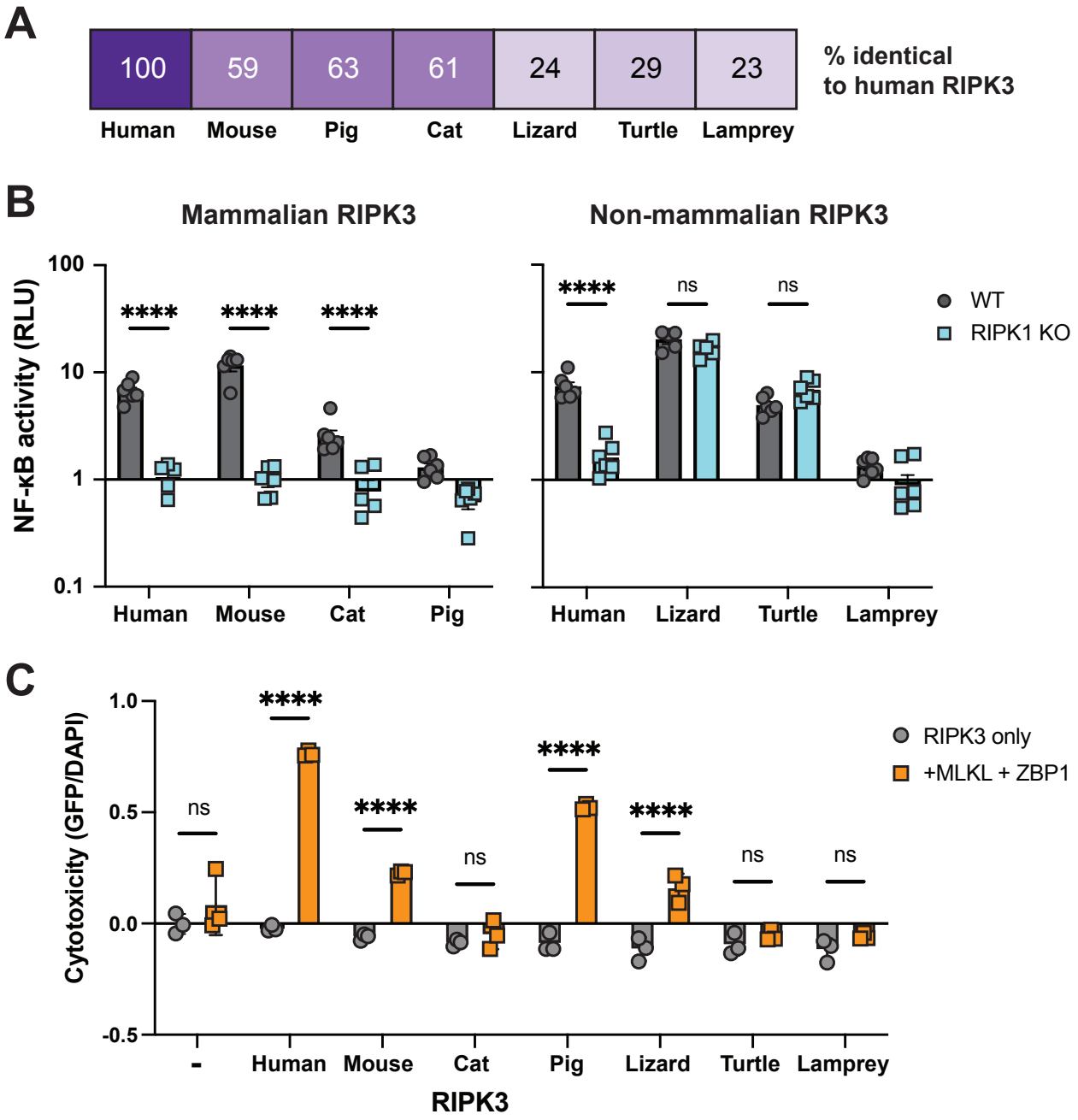

Figure 2. Diverse vertebrate RIPK3 proteins activate NF-κB. (A) Percent similarity of RIPK3 from the indicated species compared to humans. (B) RIPK3 proteins were transfected into WT or RIPK1 KO HEK293T cells, along with NF-κB firefly luciferase and control renilla luciferase reporter plasmids (see Materials and Methods), and NF-κB activity was measured at 18h post-transfection. (C) RIPK3 proteins were transfected into HEK293T cells with and without human ZBP1 and MLKL. At 18h post-transfection, cells were stained using the ReadyProbe Cell Viability kit and fluorescence was measured using a plate reader. Species shown are mouse (*Mus musculus*), cat (*Felis catus*), pig (*Sus scrofa*), lizard (*Anolis carolinensis*), turtle (*Chelonia mydas*), and lamprey (*Petromyzon marinus*). Data are representative of 3-5 independent experiments with n=3-6 replicates per group. Data were analyzed using two-way ANOVA with Šidák's multiple comparisons test. ns = not significant, **** = p<0.0001.

213 *Conservation of the RHIM sequence determines RIPK3 activation of NF-κB*

214 The conservation of NF-κB activation by RIPK3 proteins that share as little as 24%
215 sequence identity and are up to >300 million years diverged [29] suggests some regions
216 of the protein are likely highly conserved. To identify such regions, we returned to our
217 positive selection analyses. While we identified rapidly evolving sites throughout the
218 primate RIPK3, there was a cluster of sites in and around the C-terminal RHIM (Fig 3A
219 Supplementary File 5), which is a known region of interaction between RIPK1 and RIPK3
220 and RIPK3 homooligomerization [30, 31]. Intriguingly, despite multiple rapidly evolving
221 sites within the RHIM, a core tetrad (VQVG) is not rapidly evolving. Similarly, the core
222 tetrads of bat and carnivore RIPK3 are not rapidly evolving (Fig 3B). Furthermore, the
223 RIPK3 core RHIM tetrad is highly conserved across vertebrates (Fig 3C). This is despite
224 loss of other functional motifs in specific lineages, including loss of the RIPK3 catalytic
225 site in felines (Supplementary Figure 7).

226 We therefore tested whether this conserved RHIM tetrad was responsible for
227 activation of NF-kB by diverse vertebrate RIPK3s. We mutated the RIPK3 RHIM core
228 tetrad (V/I-Q-V/I-G to AAAA) in our panel of vertebrate RIPK3 proteins and tested the
229 ability of these proteins to activate NF-kB in human cells. Mutation of human, mouse, and
230 cat RIPK3 RHIMs reduced activation of NF-κB as expected (Fig 3D, Supplementary
231 Figure 5). Surprisingly, despite activating independently of RIPK1 (Fig 2B), activation of
232 NF-κB by lizard and turtle RIPK3 remains dependent on the RHIM (Fig 3E, left), and
233 independent of RIPK3 kinase activity (Supplementary Figure 8-9). These data support
234 that reptile RIPK3 activates NF-κB through a distinct mechanism from mammalian RIPK3,
235 but one that is still highly dependent on the RHIM core tetrad. Interestingly, while
236 analyzing RHIM domains of non-human RIPK3, we observed that the sea lamprey RHIM
237 diverges from the canonical V/I-Q-V/I-G tetrad and instead contains TQIG (Fig 3C). To
238 determine if this was responsible for the limited activation of NF-κB by sea lamprey
239 RIPK3, we mutated this motif to IQIG and observed an increase in NF-κB activation (Fig
240 3E, right). Altogether, these data indicate that NF-κB activation is a conserved function of
241 RIPK3 that requires conservation of the core RHIM tetrad, but allows for substantial
242 sequence divergence elsewhere in the protein.

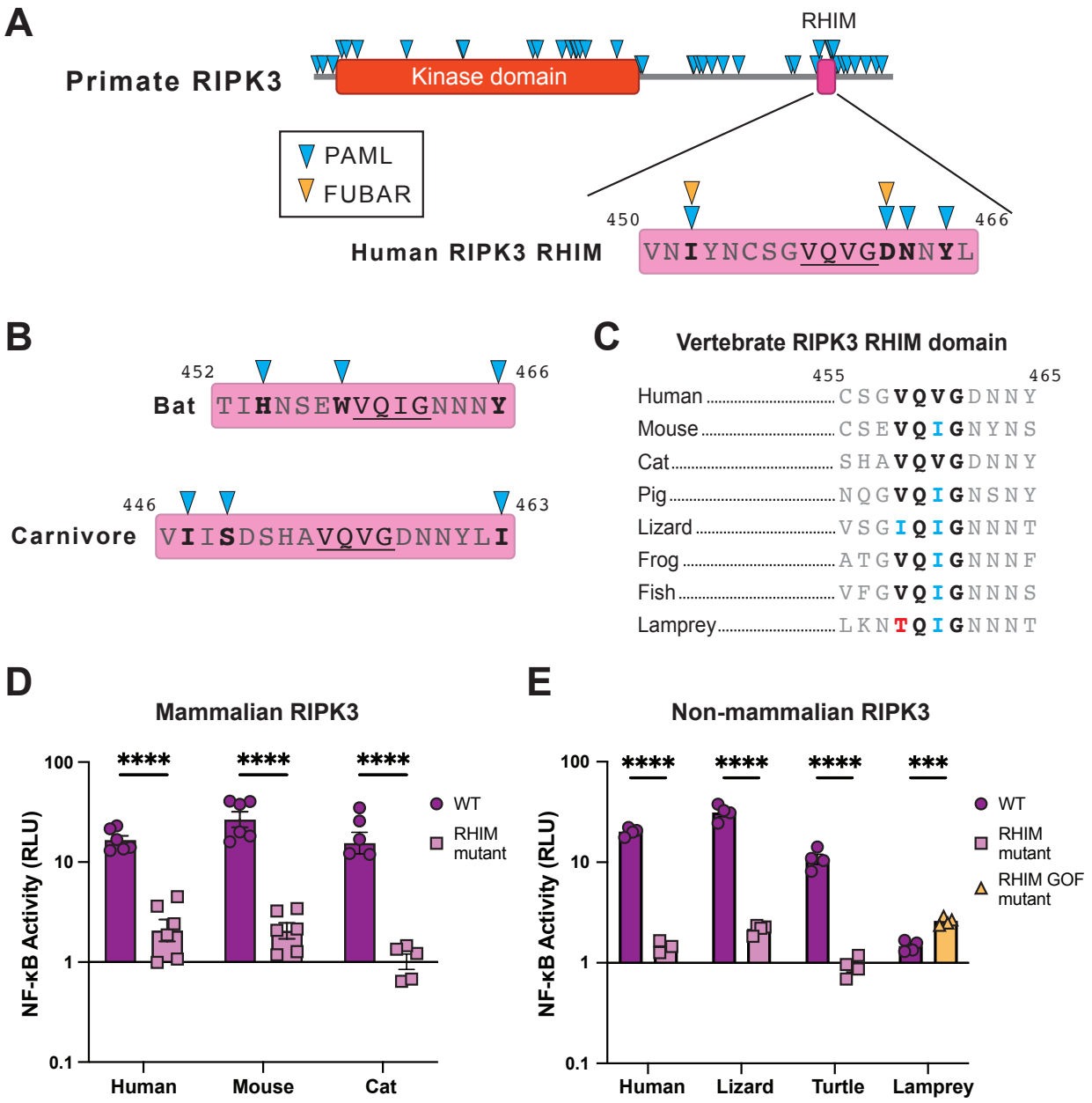

Figure 3. Conservation of the RHIM sequence determines RIPK3 NF-κB activation. A) Residues evolving under positive selection in primate RIPK3 and the primate RIPK3 RHIM domain mapped on the human sequence. (B) Residues evolving under positive selection in bat and carnivore RIPK3, mapped on to the *Sturnira hondurensis* and *Felis catus* sequences respectively. (C) Alignments of the RIPK3 RHIM across diverse vertebrates. Residue numbers refer to the human sequence. (D-E) Mammalian (D) and non-mammalian (E) RIPK3 proteins were transfected into WT HEK293T cells along with NF-κB firefly luciferase and control renilla luciferase reporter plasmids (see Materials and Methods). NF-κB activity was measured at 18h post-transfection. Species shown are mouse (*Mus musculus*), cat (*Felis catus*), pig (*Sus scrofa*), lizard (*Anolis carolinensis*), turtle (*Chelonia mydas*), and lamprey (*Petromyzon marinus*). Data are representative of 3-5 independent experiments with n=3-6 replicates per group. Data were analyzed using two-way ANOVA with Šidák's multiple comparisons test. ns = not significant, **** = p<0.0001.

257 *NF-κB activation is a shared function of RHIM-containing proteins and can be tuned by*
258 *the RHIM*

259 Given that activation of NF-κB by RIPK3 is dependent the RHIM, we hypothesized
260 that the core RHIM tetrad and activation of NF-κB would be broadly conserved across all
261 RHIM-containing proteins, including RIPK1, ZBP1 and TRIF. We found that the RIPK1
262 RHIM is highly conserved in vertebrates and in RIPK1-like protein found in zebra mussel
263 (Fig 4A). Human RIPK1 is known to activate NF-κB independently of its RHIM through
264 polyubiquitination of the intermediate domain [32, 33]. However, the strong conservation
265 of the RHIM domain tetrad sequence (V/I-Q-V/I-G) of RIPK1 across species led us to
266 hypothesize that RHIM-mediated activation of NF-κB by RIPK1 is also conserved. We
267 therefore tested a diverse panel of metazoan RIPK1 proteins in our NF-κB assay. To
268 avoid the effects of both kinase activity and kinase-mediated interactions [34], we
269 generated RIPK1 C-terminus ($RIPK1^{CT}$) proteins from diverse species (Supplementary
270 Figure 10). Both WT and RHIM mutant human $RIPK1^{CT}$ activate NF-κB to the same extent
271 as full length RIPK1 (Supplementary Figure 11), validating our use of this system to
272 characterize RIPK1 functions independent from the kinase domain. Diverse vertebrate
273 $RIPK1^{CT}$ proteins activate NF-κB independent of endogenous RIPK1 (Supplementary
274 Figure 12), consistent with our hypothesis that NF-κB activation is an ancestral and
275 conserved function of these proteins. However, like RIPK3, the specific sequence
276 requirements for RIPK1-mediated NF-κB activation varied by species. Specifically,
277 mutation of the RHIM domain does not affect activation of NF-κB by mammalian proteins,
278 including human, mouse, cat, and pig (Figure 4B, left). In contrast, mutation of the RHIM
279 domain attenuated or completely prevented the ability of non-mammalian (lizard, sea
280 lamprey, and zebra mussel) $RIPK1^{CT}$ to activate NF-κB (Figure 4B, right).

281 Other than RIPK1 and RIPK3, only two other human proteins contain a RHIM
282 domain, TRIF and ZBP1. The TRIF RHIM and the first RHIM of ZBP1 are also highly
283 conserved in mammals and some other tetrapods, whereas the second RHIM of ZBP1
284 diverges even within mammals (Fig 4C, Supplementary Figure 13A). We then tested for
285 RHIM-dependence of NF-κB activation by human TRIF and ZBP1. As described
286 previously [35], ZBP1 activates NF-κB in a RHIM- and RIPK1-dependent manner (Fig

287 4D). Consistent with our evolutionary prediction, only the first RHIM tetrad is required for
288 NF-κB activation by ZBP1 (Fig 4D). Conversely, mutation of the TRIF RHIM domain does
289 not affect activation of NF-κB, and activation is only moderately reduced in RIPK1 KO
290 cells (Supplementary Figure 13B-C), likely due to the TIR domain in TRIF that is known
291 mediate its innate immune signaling [36].

292 Finally, due to the central role of the core tetrad of the RHIM domain, we tested
293 the plasticity of RHIM function with regard to sequence divergence. In our phylogenetic
294 analyses of RIPK3, we identified several species in which the RHIM core tetrad has
295 diverged, particularly outside of tetrapods, including tetrads that have diverged from the
296 conserved motif (V/I-Q-V/I-G) at only a single residue (Supplementary Table 2). To test
297 for functional differences, we inserted these naturally-occurring RHIM tetrads into human
298 RIPK3 and characterized the ability to activate NF-κB and cell death. We included tetrads
299 found in rodents, bats, eulipotyphlans, reptiles, and fish (VQFG), amphibians and fish
300 (LQIG, VQSG), fish (CQIG), and sea lamprey (TQIG). Interestingly, while most tested
301 variants activate NF-κB compared to the inactive RIPK3 RHIM mutant (AAAA tetrad),
302 albeit lower than the WT (VQVG) tetrad, TQIG and VQSG did not activate NF-κB (Fig 4E,
303 Supplementary Figure 14-15). These data suggest that, while there is some plasticity in
304 the RHIM tetrad, not all residues are functional. All tetrad variants were able to activate
305 ZBP1-dependent cell death similar to WT RIPK3 (Fig 4F), further revealing the separation
306 of RIPK3-mediated NF-κB activation from cell death activation. Altogether, these data
307 suggest that diversity in the RIPK3 RHIM domain may tune activation of NF-κB and tailor
308 RIPK3 function to the specific needs of species.

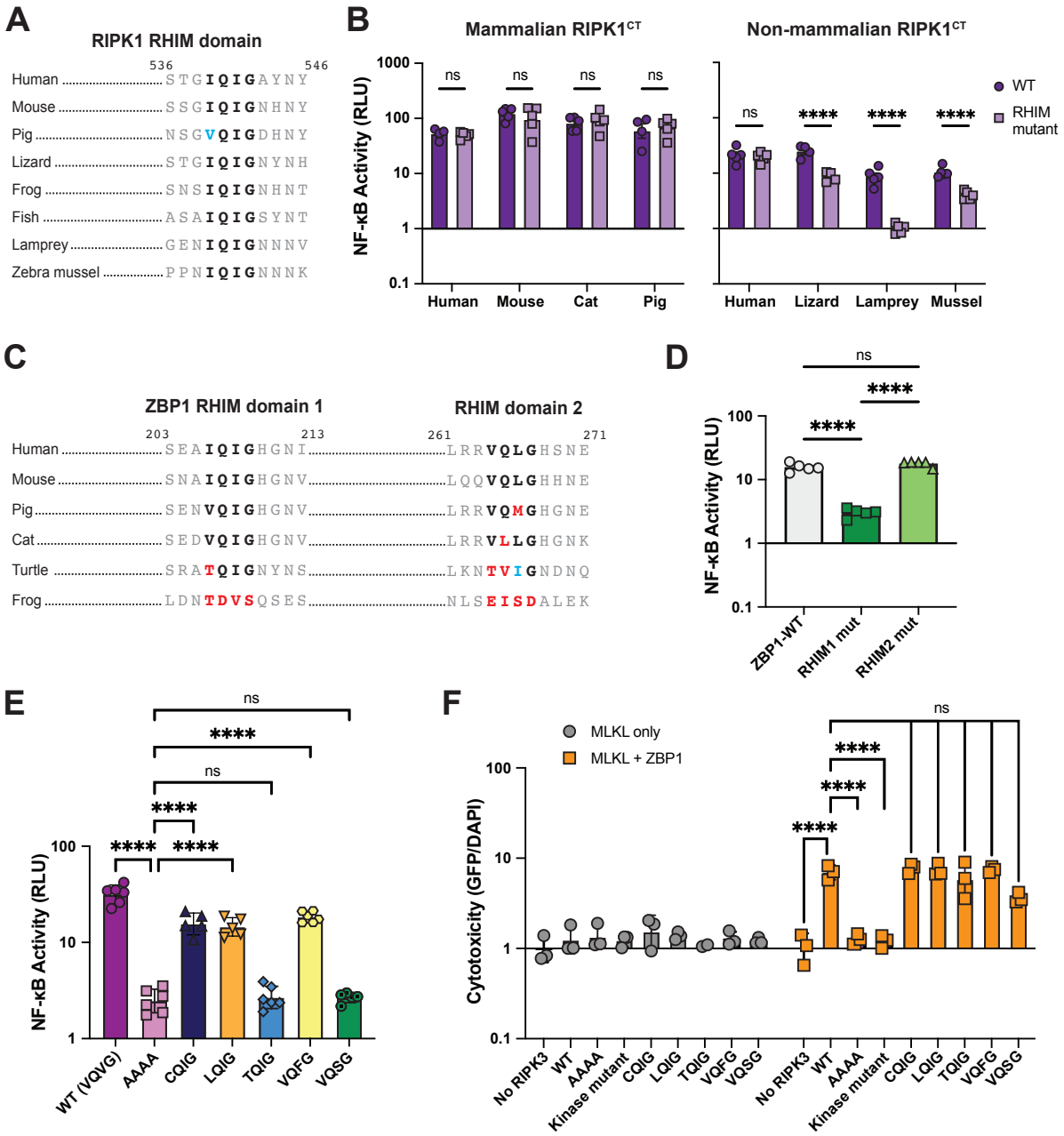

Figure 4. NF-κB activation is a shared function of RHIM-containing proteins and can be tuned by the RHIM. (A) Alignment of RIPK1 RHIM across diverse vertebrates. Residue numbers refer to the human sequence. (B) Diverse vertebrate RIPK1^{CT} proteins. were transfected into HEK293T cells along with NF-κB firefly luciferase and control renilla luciferase reporter plasmids (see Materials and Methods), and NF-κB activity was measured at 18h post-transfection. (C) Alignment of ZBP1 RHIMs across diverse vertebrates. Residue numbers refer to the human sequence. (D) Activation of NF-κB by WT and RHIM mutant ZBP1 proteins. (E) NF-κB activation by human RIPK3 with the indicated RHIM tetrad variant. (F) Human RIPK3 proteins with the indicated RHIM tetrad variants were transfected into HEK293T cells with MLKL (gray circles) or MLKL and ZBP1 (orange squares) and viability was measured at 18h post-transfection. Data are representative of 2-5 independent experiments with n=3-6 replicates per group. Data were analyzed using two-way ANOVA with Šidák's multiple comparisons test (A, D) one-way ANOVA with Tukey's multiple comparisons test (E), or two-way ANOVA with Tukey's multiple comparisons test (F). ns = not significant, **** = p<0.0001.

323 **Discussion**

324 Activation of NF-κB is critical to both the innate and adaptive immune response in
325 humans and mice [19], and is a deeply conserved pathway in many metazoans [23-25].
326 Despite this deep conservation of NF-κB signaling, differences in the function and
327 regulation of NF-κB-associated proteins between mice and humans have been identified
328 [19], suggesting that this functionally well-conserved pathway can be adapted to different
329 species. These data indicate that broader phylogenetic analysis of the genes and
330 functions that are associated with NF-κB signaling are needed to understand immune
331 responses across species, including those that harbor pathogens that pose a zoonotic
332 threat to humans.

333 Here, we apply broad phylogenetic and functional sampling to the RIP kinase family
334 of NF-κB activators. Using a phylogenomic approach, we identified widespread
335 conservation of RIPK1, RIPK2, and RIPK4 and their associated proteins within
336 vertebrates. We also show conservation of activation of NF-κB signaling by RIPK1 and
337 RIPK3 across diverse vertebrate species that is largely reliant on the highly conserved
338 core tetrad of the RHIM domains found in both proteins. This striking conservation of
339 RIPK1- and RIPK3-mediated activation of NF-κB, from species that span >500 million
340 years of vertebrate evolution, underscores the core functionality of RIP kinases as NF-κB
341 activating proteins. Despite this conservation of NF-κB activation, we also observed
342 lineage specific changes in RIPK presence or mechanisms of NF-κB activation. For
343 instance, we observed recurrent gene loss of RIPK3 and RIPK5 throughout the vertebrate
344 phylogeny, and discovered a second paralog of RIPK2 in many non-mammalian
345 vertebrate species (RIPK2B). In addition, although RIPK3-mediated activation of NF-κB
346 is highly dependent on RIPK1 across diverse mammals, RIPK3 activation of NF-κB in
347 reptiles is independent of RIPK1. Activation of NF-κB is part of the antiviral immune
348 response and is known to be antagonized by viruses across a range of species, including
349 vertebrates and non-vertebrates [37-39]. This antagonism could result in adaptation of
350 NF-κB-associated proteins, including RIP kinases, leading to lineage-specific
351 mechanisms of activation that are tailored to the specific contexts within and between
352 species.

353 The most striking differences in RIPK-associated genes and functions are those
354 involved in necroptosis. Necroptosis is highly inflammatory and the associated proteins
355 must therefore be tightly regulated, as it could be a cause of immunopathology during
356 infection. Despite this, necroptosis has been shown to be important for the response to
357 several viruses [40-42]. It is hypothesized that necroptosis, defined by RIPK3-mediated
358 activation of MLKL, arose in vertebrates [8, 43]. Interestingly, we find that two critical
359 regulators of necroptosis, CASP8 and ZBP1, are only found in tetrapods, suggestive of
360 an additional innovation within the necroptosis pathway during the divergence of
361 tetrapods. Moreover, consistent with previous observations [8, 9], we observe a large
362 number of necroptosis-associated gene losses, while also discovering important
363 functional motifs in necroptosis proteins in distinct tetrapod lineages. These data support
364 a model where necroptosis has been constructed as an important facet of the innate
365 immune response in some tetrapods, but is not universal and has been deconstructed in
366 species where the immunopathologic effects outweigh the benefits.
367 There have been several hypotheses to explain the loss of necroptosis associated
368 proteins in specific vertebrate lineages, such as diet (*e.g.,* carnivores) or behavior (*e.g.,*
369 torpor in reptiles) [8]. While the cause of a specific instance of gene loss is difficult to
370 identify, it is clear that gene loss can provide an evolutionary tool for adaptation [44].For
371 example, caspases, which are key regulators of both immunologically silent apoptosis
372 and inflammatory pyroptosis, differ greatly across mammals, with lineage-specific
373 caspase repertoires including both loss and gain of novel caspases [27]. Even within a
374 single mammalian order, homologous caspases have been found to serve different
375 functions in response to pathogens [45]. This type of lineage-specific innovation likely
376 exists for necroptosis, and gene loss could be a cause or a result of adaptations. Indeed,
377 differences in MLKL activation by RIPK3 across species have been identified [46], which
378 may be the result of additional diverse regulatory mechanisms for necroptosis even
379 amongst species with an intact pathway. Strikingly, despite the lack of a complete
380 necroptosis pathway in some lineages (cat, turtle, lamprey), our functional data indicate
381 that RIPK3 retains the ability to activate NF-κB. Activation of NF-κB could therefore
382 represent the ancestral function of RIPK3, and it has been co-opted to activate
383 necroptosis in vertebrates.

384 The RHIM core tetrad was previously known to be conserved between humans and
385 mice [47]. Here, we expand this analysis and identify striking conservation of the RIPK3,
386 RIPK1, ZBP1, and TRIF RHIM domains across most vertebrates. While activation of NF-
387 κB by all tested non-human RIPK3 proteins was highly dependent on the RHIM domain,
388 only non-mammalian RIPK1^{CT} proteins required the RHIM for maximal NF-κB activation.
389 These species (lizard, lamprey, and zebra mussel) also lack ZBP1, with lamprey and
390 zebra mussel predating the emergence of ZBP1 in tetrapods. Necroptosis may have
391 driven evolution of RHIM-independent activation of NF-κB by RIPK1. This may have also
392 shaped RHIM-dependent functions of RIPK3 across vertebrates, as the RHIM tetrad is
393 much less conserved in fish compared to tetrapods, and insertion of these tetrad variants
394 into human RIPK3 alters its function. Virus antagonism has also likely played a role in the
395 evolution of RIPK3 and RIPK1 function. For example, vaccinia virus E3 prevents Z-DNA
396 sensing by ZBP1 [40], human cytomegalovirus UL36 promotes MLKL degradation, and
397 poxviruses encode an MLKL homolog to prevent RIPK3-mediated activation of host MLKL
398 [48]. Conservation of the RHIM domain may be a way to retain some RIPK3/RIPK1 innate
399 immune functions in the face of such antagonism. However, several viruses have taken
400 advantage of this conservation and encode RHIM-containing proteins to prevent RHIM-
401 dependent functions [43, 47]. Intriguingly, several of these mechanisms are known to be
402 species-specific and differ between humans and mice [13, 14]. These data support a
403 model where viruses and host necroptosis are engaged in a molecular arms race that has
404 shaped the function of RIPK3 and RIPK1 across vertebrate species.

405 Altogether, our combined phylogenetic and functional approaches reveal both
406 conservation and a striking lack of conservation in vertebrate RIPKs and their associated
407 proteins and functions. Such characteristics are common hallmarks of pathways that are
408 required for the innate immune response to pathogens, but are under constant
409 evolutionary pressure to innovate to avoid pathogen antagonism. The strong conservation
410 of NF-κB activation by RIPK1 across species is consistent with the model in which RIPK1
411 function is central to determining cell fate downstream of TNF and TLR signaling [49].
412 Moreover, because some pathogens have evolved strategies to inhibit CASP8, RIPK3-
413 and RIPK1-mediated necroptosis is activated as a secondary cell death strategy when
414 CASP8 is inhibited [50]. This places both RIPK3 and RIPK1, critical regulators of

415 necroptosis, at the center of determining cell fate during pathogen infection. The
416 divergence of RIPK3 and RIPK1 across vertebrates identified here, as well as the
417 previous finding that these proteins are evolving under positive selection [9, 16, 17],
418 reveals that pathogens are likely the driving force behind the lineage-specific regulatory
419 mechanisms or functions of these proteins across species that we observe here. Thus,
420 the functional divergence identified in our work highlights the evolutionary innovation that
421 can arise in innate signaling pathways across diverse species, and underscores the
422 importance of considering natural diversity when characterizing the innate immune
423 response to pathogens.
424

425 **Materials & Methods**

426 *Positive selection analysis*

427 Positive selection analysis was performed using three independent methods as we have
428 done previously [51, 52]. Nucleotide sequences from the indicated mammalian clade that
429 aligned to full-length human RIPK1-5 were downloaded from NCBI and aligned using
430 ClustalOmega [53]. Maximum likelihood (ML) tests were performed with codeml in the
431 PAML software suite [54]. For PAML, aligned sequences were subjected to ML tests
432 using NS sites models disallowing (M7) or allowing (M8) positive selection. The reported
433 p-values were calculated using a chi-squared test on twice the difference of the log
434 likelihood (lnL) values between the two models using 2 degrees of freedom. We confirmed
435 convergence of lnL values by performing each analysis using two starting omega (dN/dS)
436 values (0.4 and 1.5). Codons evolving under positive selection from PAML analyses have
437 a posterior probability greater than 0.90 using Native Empirical Bayes (NEB) and Bayes
438 Empirical Bayes (BEB) analysis and the F61 codon frequency model. The same
439 nucleotide alignments were used as input for FUBAR [55] and MEME [56] using the
440 DataMonkey server [57]. In both cases, default parameters were used and codons with a
441 signature of positive selection with a p-value of <0.01 are reported. Accession numbers
442 for input sequences, PAML p-values, and sites identified can be found in Supplementary
443 Files 1-3.
444

445 *Gene loss analysis*

446 Using the aligned and filtered vertebrate RIPK sequences (4,550 sequences in
447 total, see 'Phylogenetic analysis' section), a tree was built using FastTree [58, 59]
448 implemented using Geneious. Using this tree, we were able to identify and extract *bona*
449 *fide* RIP kinases and remove similar, non-RIP kinases. The extracted sequences were
450 again aligned using Clustal Omega and filtered using the criteria above (See
451 'Phylogenetic analysis' section). A second tree was generated using FastTree. From this
452 tree, we extracted individual sequence lists for RIPK1-5 to determine which vertebrate
453 species did or did not have each RIPK. This method was repeated for CASP2 and
454 CASP8-10, ZBP1, MLKL, TRIF, FADD, NOD 1 and 2, and IRF6. The list of species and
455 lists of accession numbers for each protein can be found in Supplementary Files 4 and 5.
456
457 *Plasmids and constructs*
458 Coding sequences for human RIPK1 (Addgene #78834), human RIPK2
459 (ORFeome ID #4886), human RIPK3 (Addgene #78804), mouse RIPK1 (Addgene
460 #115341), and mouse RIPK3 (Addgene #78805) were cloned into apcDNA5/FRT/TO
461 backbone (Invitrogen, Carlsbad, CA) with an N-terminal V5 tag and linker using Gibson
462 Assembly (New England Biolabs, Ipswich, MA). Human RIPK4 (NP_065690.2) and
463 RIPK5 (NP_848605.1), and non-human RIPK1 C-termini (cat, XP_023109490.2; pig,
464 XP_003128209.1; chicken, NP_989733.3; lizard, XP_003224434.1; lamprey,
465 XP_032813622.1; zebra mussel, XP_052232845.1) and RIPK3 (cat, XP_003987615.3;
466 pig, XP_001927459.3; lizard, XP_003223896.2; turtle, XP_037771912.1; lamprey,
467 XP_032816533.1) homologues were ordered from Twist Biosciences (San Francisco,
468 CA, USA) and were cloned along with RHIM mutants targeting the core tetrad into the
469 pcDNA5/FRT/TO backbone (Invitrogen, Carlsbad, CA) with an N-terminal V5 tag and
470 linker using Gibson Assembly (New England Biolabs, Ipswich, MA). Kinase mutants for
471 human proteins RIPK1 (D138N), RIPK2 (D146N), RIPK3 (D142N), RIPK4 (D143N), and
472 RIPK5 (D145N), and RHIM mutants for RIPK1 (IQIG542AAAA) and RIPK3
473 (VQVG461AAAA) were generated using Gibson Assembly.
474
475 *Cell culture and transient transfections*

476 HEK293T cells (obtained from ATCC) and the generated HEK293T RIPK1 KO cells
477 were maintained at a low passage number to maintain less than one year since
478 purchase, acquisition, or generation. Both cell lines were grown in complete media
479 containing DMEM (Gibco, Carlsbad, CA), 10% FBS (Peak Serum, Wellington, CO), and
480 1% penicillin/streptomycin (Gibco, Carlsbad, CA). A day prior to transfection, HEK293T
481 and RIPK1 KO cells were seeded into 24-well plates with 500 µL complete media or 96-
482 well plates with 80 µL complete media. Cells were transiently transfected with 500 ng
483 total DNA and 1.5 µL of TransIT-X2 (Mirus Bio, Madison, WI) in 100 µL Opti-MEM
484 (Gibco, Carlsbad, CA) for a 24-well plate or 100 ng DNA and 0.3 µL TransIT-X2 in 10
485 µL Opti-MEM for a 96-well plate. DNA and TransIT-X2 were incubated at room
486 temperature for 25-30 minutes, then added dropwise to the appropriate well. Cells were
487 harvested or analyzed at 18-22 hours post-transfection.
488
489 *Generation of knockout cell lines*
490 RIPK1 knockout HEK293T cells were generated using CRISPR/Cas9 as
491 previously described [52, 60]. Briefly, plasmids were generated order to produce
492 lentivirus-like particles containing the CRISPR/Cas9 machinery and guide RNA targeting
493 exon 5 (ENSE00003586162) of RIPK1. The protocol for the molecular cloning of this
494 plasmid was adapted from Feng Zhang (Sanjana et al., 2014) using the transfer plasmid
495 pLB-Cas9 (gift from Feng Zhang, Addgene plasmid # 52962). We designed the gRNA
496 target sequence using the web tool CHOPCHOP (Labun et al., 2016), available at
497 https://chopchop.cbu.uib.no/, and synthesized oligonucleotides from Integrated DNA
498 Technologies (San Diego, CA). The synthesized oligonucleotide pair was phosphorylated
499 and annealed using T4 Polynucleotide Kinase (NEB M0201S) with T4 Ligation Buffer
500 (NEB). Duplexed oligonucleotides were ligated into dephosphorylated and BsmBI-
501 digested pLB-Cas9 using the Quick Ligase kit (NEB M2200S) to generate transfer
502 plasmid with RIPK1 guide sequence. To generate lentivirus-like particles, this transfer
503 plasmid was transfected alongside two packaging plasmids, pMD2.G (gift from Didier
504 Trono, Addgene plasmid # 12259) and psPAX2 (gift from Didier Trono, Addgene plasmid
505 # 12260), into HEK293T cells with a 1:1:1 stoichiometry. Forty-eight hours post-
506 transfection supernatant was harvested and syringe-filtered (0.45µm). Supernatant

507 containing sgRNA-encoding lentivirus-like particles was then used to transduce HEK293T
508 cells. Transduced cells were cultured in growth media for 48 hours, then cultured in
509 growth media supplemented with 1 µg/ml puromycin for 72 hours. Using limiting dilution
510 in 96-well plates, the monoclonal cell line was then obtained. RIPK1 knockout was
511 confirmed by Sanger sequencing and by western blot using an α-RIPK1 antibody.
512
513 *NF-κB and IFN luciferase reporter assays*
514 To quantify NF-κB and IFN activation, we used the Dual-Glo Luciferase Assay
515 System E2920 (Promega, USA). WT or RIPK1 KO HEK293T cells were seeded in a white
516 96-well plate and transfected with firefly luciferase fused to either the NF-κB response
517 element (pGL4.32, Promega) or the human IFN-beta promoter (IFN-Beta-pGL3, Addgene
518 #102597), renilla luciferase fused to herpes simplex virus thymidine kinase promoter
519 (pTK-Renilla, Thermo Scientific), and the indicated RIPK. Firefly luciferase was used as
520 the primary reporter with renilla luciferase being a normalization control. Eighteen to 24
521 hours after transfection, Dual-Glo Luciferase Assay Reagent was added to each
522 transfected well as well as 3-6 untransfected wells to serve as a negative control.
523 Following a 10-minute incubation, the firefly luciferase signal was measured using a
524 BioTek Cytation imaging reader with Gen5 software (Agilent Technologies, San Diego,
525 CA). Then, Dual-Glo Stop & Glo reagent was added to each well. Following a 10-minute
526 incubation, the renilla luciferase signal was measured. The background luminescence
527 signal from the buffer-treated untransfected conditions was subtracted from other
528 conditions, firefly values were normalized to renilla values, and all samples were
529 normalized to the empty vector control condition. Values are reported as NF-κB activity
530 (firefly/renilla).
531
532 *Cell death assay*
533 Cell viability was measured using the ReadyProbes Cell Viability Imaging Kit, Blue/Green
534 (ThermoFisher Scientific). HEK293T cells were seeded in 80 µL of DMEM+/+ (See "Cell
535 culture and transient transfections") in a clear 96-well plate and transfected with the
536 indicated plasmids or a vector control. Eighteen hours post-transfection, cells were
537 stained using NucBlue Live reagent, which stains all nuclei, and NucGreen Dead reagent,

538 which stains only dead cells. A 2x concentrated mix (4 drops/mL of each dye) was made
539 and added to wells to 1x concentration. Cells were incubated for 20 minutes at room
540 temperature. Fluorescence for NucBlue (DAPI, excitation 377/20, emission 447/20) and
541 NucGreen (GFP, excitation 469/20, emission 525/20) were read using a BioTek Cytation
542 imaging reader with Gen5 software (Agilent Technologies, San Diego, CA). Unstained
543 wells were read and used as controls for background fluorescence. GFP values were
544 normalized to DAPI values, and all samples were normalized to the vector control
545 condition. Values are reported as Cytotoxicity (GFP/DAPI).
546
547 *Immunoblotting and antibodies*
548 Eighteen to 22 hours post-transfection, cells were washed with 1X PBS and lysed with
549 boiling 1x NuPAGE LDS sample buffer containing 5% β-mercaptoethanol at room
550 temperature for 5 minutes and then at 98°C for 7-10 minutes. Lysates were separated
551 by SDS-PAGE (4-15% Bis-tris gel; Life Technologies, San Diego, CA) with 1X MOPS
552 buffer (Life Technologies, San Diego, CA). Proteins were transferred onto a
553 nitrocellulose membrane (Life Technologies, San Diego, CA) and blocked with PBS–T
554 containing 5% bovine serum albumin (BSA) (Spectrum, New Brunswick, NJ).
555 Membranes were incubated with the indicated rabbit primary antibodies diluted with 5%
556 BSA and PBS-T at 1:1000 overnight at 4°C (α-V5 clone D3H8Q, α-GAPDH clone
557 14C10, α-RIPK1 clone E8S7U XP, α-RIPK2 clone D10B11, α-RIPK3 clone E1Z1D, α-
558 RIPK4 #12636; Cell Signaling Technology, Danvers, MA). Membranes were rinsed
559 three times with PBS-T, incubated with HRP-conjugated rabbit secondary antibody
560 diluted at 1:10,000 with 5% BSA and PBS-T for 30 minutes at room temperature, and
561 developed with SuperSignal West Pico PLUS Chemiluminescent Substrate (Thermo
562 Fisher Scientific, Carlsbad, CA).
563
564 *Statistical analysis*
565 Statistical analyses were completed using GraphPad Prism 10 software. Tests were
566 performed as indicated. Error bars were calculated using SEM.
567
568 **Acknowledgements**

This work was supported by National Institutes of Health grant R35 GM133633 (to MDD); Pew Biomedical Scholars Program (to MDD); Burroughs Wellcome Investigators in the Pathogenesis of Infectious Disease Program (to MDD); and BrightSpinnaker Fellowship (to CMR). We thank all members of the Daugherty lab for helpful discussions and Scott Biering, Ryan Langlois, and Patrick Mitchell for their critical reading of this manuscript.

Conflict of Interest

The authors declare that they have no conflict of interest.

References

1. Newton, K., *RIPK1 and RIPK3: critical regulators of inflammation and cell death.* Trends Cell Biol, 2015. **25**(6): p. 347-53.
2. Sun, L., et al., *Mixed lineage kinase domain-like protein mediates necrosis signaling downstream of RIP3 kinase.* Cell, 2012. **148**(1-2): p. 213-27.
3. Wang, L., F. Du, and X. Wang, *TNF-alpha induces two distinct caspase-8 activation pathways.* Cell, 2008. **133**(4): p. 693-703.
4. Mandal, P., et al., *RIP3 induces apoptosis independent of pronecrotic kinase activity.* Mol Cell, 2014. **56**(4): p. 481-95.
5. Meylan, E., et al., *RIP1 is an essential mediator of Toll-like receptor 3-induced NF-kappa B activation.* Nat Immunol, 2004. **5**(5): p. 503-7.
6. Moriwaki, K., et al., *The necroptosis adaptor RIPK3 promotes injury-induced cytokine expression and tissue repair.* Immunity, 2014. **41**(4): p. 567-78.
7. Orozco, S. and A. Oberst, *RIPK3 in cell death and inflammation: the good, the bad, and the ugly.* Immunol Rev, 2017. **277**(1): p. 102-112.
8. Dondelinger, Y., et al., *An evolutionary perspective on the necroptotic pathway.* Trends Cell Biol, 2016. **26**(10): p. 721-732.
9. Agueda-Pinto, A., et al., *Convergent Loss of the Necroptosis Pathway in Disparate Mammalian Lineages Shapes Viruses Countermeasures.* Front Immunol, 2021. **12**: p. 747737.
10. Harris, K.G., et al., *RIP3 Regulates Autophagy and Promotes Coxsackievirus B3 Infection of Intestinal Epithelial Cells.* Cell Host Microbe, 2015. **18**(2): p. 221-32.
11. Croft, S.N., E.J. Walker, and R. Ghildyal, *Human Rhinovirus 3C protease cleaves RIPK1, concurrent with caspase 8 activation.* Sci Rep, 2018. **8**(1): p. 1569.
12. Wagner, R.N., J.C. Reed, and S.K. Chanda, *HIV-1 protease cleaves the serine-threonine kinases RIPK1 and RIPK2.* Retrovirology, 2015. **12**: p. 74.
13. Muscolino, E., et al., *Species-Specific Inhibition of Necroptosis by HCMV UL36.* Viruses, 2021. **13**(11).
14. Huang, Z., et al., *RIP1/RIP3 binding to HSV-1 ICP6 initiates necroptosis to restrict virus propagation in mice.* Cell Host Microbe, 2015. **17**(2): p. 229-42.

609 15. Liu, X., et al., *Epstein-Barr virus encoded latent membrane protein 1 suppresses*
610 *necroptosis through targeting RIPK1/3 ubiquitination.* Cell Death Dis, 2018. **9**(2):
611 p. 53.
612 16. Palmer, S., et al., *Evolutionary profile for (host and viral) MLKL indicates its*
613 *activities as a battlefront for extensive counteradaptation.* Mol Biol Evol, 2021.
614 **38**(12): p. 5405-522.
615 17. Cariou, M., et al., *Distinct evolutionary trajectories of SARS-CoV-2-interacting*
616 *proteins in bats and primates identify important host determinants of COVID-19.*
617 Proc Natl Acad Sci U S A, 2022. **119**(35): p. e2206610119.
618 18. Daugherty, M.D. and H.S. Malik, *Rules of engagement: molecular insights from*
619 *host-virus arms races.* Annu Rev Genet, 2012. **46**: p. 677-700.
620 19. Zhang, Q., M.J. Lenardo, and D. Baltimore, *30 Years of NF-kappaB: A Blossoming*
621 *of Relevance to Human Pathobiology.* Cell, 2017. **168**(1-2): p. 37-57.
622 20. Cuny, G.D. and A. Degterev, *RIPK protein kinase family: Atypical lives of typical*
623 *kinases.* Semin Cell Dev Biol, 2021. **109**: p. 96-105.
624 21. Eng, V.V., M.A. Wemyss, and J.S. Pearson, *The diverse roles of RIP kinases in*
625 *host-pathogen interactions.* Semin Cell Dev Biol, 2021. **109**: p. 125-143.
626 22. Lv, S., et al., *Comparative and evolutionary analysis of RIP kinases in immune*
627 *responses.* Front Genet, 2022. **13**: p. 796291.
628 23. Wang, X.W., et al., *Evidence for the ancient origin of the NF-kappaB/IkappaB*
629 *cascade: its archaic role in pathogen infection and immunity.* Proc Natl Acad Sci U
630 S A, 2006. **103**(11): p. 4204-9.
631 24. Hetru, C. and J.A. Hoffmann, *NF-kappaB in the immune response of Drosophila.*
632 Cold Spring Harb Perspect Biol, 2009. **1**(6): p. a000232.
633 25. Williams, L.M. and T.D. Gilmore, *Looking Down on NF-kappaB.* Mol Cell Biol,
634 2020. **40**(15).
635 26. Rodriguez, D.A., et al., *Caspase-8 and FADD prevent spontaneous ZBP1*
636 *expression and necroptosis.* Proc Natl Acad Sci U S A, 2022. **119**(41): p.
637 e2207240119.
638 27. Eckhart, L., et al., *Identification of novel mammalian caspases reveals an important*
639 *role of gene loss in shaping the human caspase repertoire.* Mol Biol Evol, 2008.
640 **25**(5): p. 831-41.
641 28. Yatim, N., et al., *RIPK1 and NF-kappaB signaling in dying cells determines cross-*
642 *priming of CD8(+) T cells.* Science, 2015. **350**(6258): p. 328-34.
643 29. Benton, M.J. and P.C. Donoghue, *Paleontological evidence to date the tree of life.*
644 Mol Biol Evol, 2007. **24**(1): p. 26-53.
645 30. Wu, X., et al., *The structure of a minimum amyloid fibril core formed by necroptosis-*
646 *mediating RHIM of human RIPK3.* Proc Natl Acad Sci U S A, 2021. **118**(14).
647 31. Sun, X., et al., *Identification of a novel homotypic interaction motif required for the*
648 *phosphorylation of receptor-interacting protein (RIP) by RIP3.* J Biol Chem, 2002.
649 **277**(11): p. 9505-11.
650 32. Li, H., et al., *Ubiquitination of RIP is required for tumor necrosis factor alpha-*
651 *induced NF-kappaB activation.* J Biol Chem, 2006. **281**(19): p. 13636-13643.
652 33. Ea, C.K., et al., *Activation of IKK by TNFalpha requires site-specific ubiquitination*
653 *of RIP1 and polyubiquitin binding by NEMO.* Mol Cell, 2006. **22**(2): p. 245-57.

654 34. Delanghe, T., Y. Dondelinger, and M.J.M. Bertrand, *RIPK1 Kinase-Dependent*
655 *Death: A Symphony of Phosphorylation Events.* Trends Cell Biol, 2020. **30**(3): p.
656 189-200.
657 35. Rebsamen, M., et al., *DAI/ZBP1 recruits RIP1 and RIP3 through RIP homotypic*
658 *interaction motifs to activate NF-kappaB.* EMBO Rep, 2009. **10**(8): p. 916-22.
659 36. Nanson, J.D., B. Kobe, and T. Ve, *Death, TIR, and RHIM: Self-assembling*
660 *domains involved in innate immunity and cell-death signaling.* J Leukoc Biol, 2019.
661 **105**(2): p. 363-375.
662 37. Albarnaz, J.D., et al., *Molecular mimicry of NF-kappaB by vaccinia virus protein*
663 *enables selective inhibition of antiviral responses.* Nat Microbiol, 2022. **7**(1): p.
664 154-168.
665 38. Gonzalez Lopez Ledesma, M.M., et al., *Dengue virus NS5 degrades ERC1 during*
666 *infection to antagonize NF-kB activation.* Proc Natl Acad Sci U S A, 2023. **120**(23):
667 p. e2220005120.
668 39. Palmer, W.H., et al., *Induction and Suppression of NF-kappaB Signalling by a DNA*
669 *Virus of Drosophila.* J Virol, 2019. **93**(3).
670 40. Koehler, H., et al., *Vaccinia virus E3 prevents sensing of Z-RNA to block ZBP1-*
671 *dependent necroptosis.* Cell Host Microbe, 2021. **29**(8): p. 1266-1276 e5.
672 41. Balachandran, S. and G.F. Rall, *Benefits and Perils of Necroptosis in Influenza*
673 *Virus Infection.* J Virol, 2020. **94**(9).
674 42. Shubina, M., et al., *Necroptosis restricts influenza A virus as a stand-alone cell*
675 *death mechanism.* J Exp Med, 2020. **217**(11).
676 43. Tummers, B. and D.R. Green, *The evolution of regulated cell death pathways in*
677 *animals and their evasion by pathogens.* Physiol Rev, 2022. **102**(1): p. 411-454.
678 44. Albalat, R. and C. Canestro, *Evolution by gene loss.* Nat Rev Genet, 2016. **17**(7):
679 p. 379-91.
680 45. Devant, P., A. Cao, and J.C. Kagan, *Evolution-inspired redesign of the LPS*
681 *receptor caspase-4 into an interleukin-1beta converting enzyme.* Sci Immunol,
682 2021. **6**(62).
683 46. Tanzer, M.C., et al., *Evolutionary divergence of the necroptosis effector MLKL.* Cell
684 Death Differ, 2016. **23**(7): p. 1185-97.
685 47. Riebeling, T., U. Kunzendorf, and S. Krautwald, *The role of RHIM in necroptosis.*
686 Biochem Soc Trans, 2022. **50**(4): p. 1197-1205.
687 48. Petrie, E.J., et al., *Viral MLKL Homologs Subvert Necroptotic Cell Death by*
688 *Sequestering Cellular RIPK3.* Cell Rep, 2019. **28**(13): p. 3309-3319 e5.
689 49. Clucas, J. and P. Meier, *Roles of RIPK1 as a stress sentinel coordinating cell*
690 *survival and immunogenic cell death.* Nat Rev Mol Cell Biol, 2023. **24**(11): p. 835-
691 852.
692 50. Remick, B.C., M.M. Gaidt, and R.E. Vance, *Effector-Triggered Immunity.* Annu
693 Rev Immunol, 2023. **41**: p. 453-481.
694 51. Tsu, B.V., et al., *Host-specific sensing of coronaviruses and picornaviruses by the*
695 *CARD8 inflammasome.* PLoS Biol, 2023. **21**(6): p. e3002144.
696 52. Stevens, D.A., et al., *Antiviral function and viral antagonism of the rapidly evolving*
697 *dynein activating adaptor NINL.* Elife, 2022. **11**.
698 53. Sievers, F., et al., *Fast, scalable generation of high-quality protein multiple*
699 *sequence alignments using Clustal Omega.* Mol Syst Biol, 2011. **7**: p. 539.

700 54. Yang, Z., *PAML 4: phylogenetic analysis by maximum likelihood.* Mol Biol Evol,
701 2007. **24**(8): p. 1586-91.
702 55. Murrell, B., et al., *FUBAR: a fast, unconstrained bayesian approximation for*
703 *inferring selection.* Mol Biol Evol, 2013. **30**(5): p. 1196-205.
704 56. Murrell, B., et al., *Detecting individual sites subject to episodic diversifying*
705 *selection.* PLoS Genet, 2012. **8**(7): p. e1002764.
706 57. Weaver, S., et al., *Datamonkey 2.0: A Modern Web Application for Characterizing*
707 *Selective and Other Evolutionary Processes.* Mol Biol Evol, 2018. **35**(3): p. 773-
708 777.
709 58. Price, M.N., P.S. Dehal, and A.P. Arkin, *FastTree: computing large minimum*
710 *evolution trees with profiles instead of a distance matrix.* Mol Biol Evol, 2009. **26**(7):
711 p. 1641-50.
712 59. Price, M.N., P.S. Dehal, and A.P. Arkin, *FastTree 2--approximately maximum-*
713 *likelihood trees for large alignments.* PLoS One, 2010. **5**(3): p. e9490.
714 60. Tsu, B.V., et al., *Diverse viral proteases activate the NLRP1 inflammasome.* Elife,
715 2021. **10**.
716